



Universität Potsdam

Olaf Schmidtman, Fred Feudel, Norbert Seehafer

## Nonlinear Galerkin methods for the 3D magnetohydrodynamic equations

NLD Preprints ; 35

# NONLINEAR GALERKIN METHODS FOR THE 3D MAGNETOHYDRODYNAMIC EQUATIONS

OLAF SCHMIDTMANN, FRED FEUDEL and NORBERT SEEHAFFER  
*Max-Planck-Gruppe Nichtlineare Dynamik, Universität Potsdam,  
PF 601553, D-14415 Potsdam, Germany*

Received .....14. January 1997

## Abstract

The usage of nonlinear Galerkin methods for the numerical solution of partial differential equations is demonstrated by treating an example. We describe the implementation of a nonlinear Galerkin method based on an approximate inertial manifold for the 3D magnetohydrodynamic equations and compare its efficiency with the linear Galerkin approximation. Special bifurcation points, time-averaged values of energy and enstrophy as well as Kaplan–Yorke dimensions are calculated for both schemes in order to estimate the number of modes necessary to correctly describe the behavior of the exact solutions.

## 1 Introduction

Nonlinear Galerkin methods are new numerical methods which have been introduced recently by Temam and Marion in connection with the theory of inertial manifolds (IMs) and approximate inertial manifolds (AIMs) to study the long-term behavior of dissipative partial differential equations (PDEs) (see e.g., Marion & Temam [1989]).

The essential aim when using these methods is to characterize nonlinear equations of high (infinite) dimension by low-dimensional equations without losing the qualitative properties, that means the long-term behavior of solutions, of the original high-dimensional system. It is important to find such low-dimensional approximations, since the numerical computation of the high-dimensional problem is impossible in many cases with currently available computer capacities. We have developed such low-dimensional approximations to investigate numerically the long-term behavior of solutions to the magnetohydrodynamic (MHD) equations.

The investigation of infinite-dimensional systems by estimating the dimensions of their global attractors has led to a progress in understanding the long-term behavior of solutions of a broad class of PDEs, including the 2D Navier–Stokes equations (NSE) [Temam, 1988]. For the 2D NSE and in case of some assumptions on the regularity of solutions for the 3D NSE it is shown that the global attractor has a finite fractal dimension [Constantin & Foias, 1985; Constantin *et al.*, 1985; Temam, 1995]. However, the finiteness of the fractal dimension of the global attractor does not imply the existence of a finite set of ordinary differential equations (ODEs) which capture the qualitative behavior of solutions to the original infinite-dimensional problem. The existence of such a finite set of ODEs is more relevant for numerical investigations than the existence of a finite-dimensional attractor.

In numerical investigations of problems described by PDEs, the original infinite-dimensional system is often approximated by a finite dimensional systems of ODEs. For instance in the case of a Fourier decomposition, the solutions are expanded with respect to eigenfunctions of the linearized operator providing a system of infinitely many ODEs for the Fourier coefficients. Although the resulting state space for the solution is still infinite-dimensional, one has to approximate this system by a truncation to a finite-dimensional one for practically calculating solutions

of the equation on a computer. Unfortunately there are no general criteria to decide whether the qualitative behavior of solutions to the infinite-dimensional problem is captured by a finite number of ODEs. In practice, one increases the number of ODEs gradually up to a number of equations for which certain quantitative characteristics of the solution reach a saturation.

An important property of dissipative systems is that after a transient period the system converges to an attractor. The number of independent Fourier modes is drastically reduced during this process. That means that in order to describe the long-term behavior of solutions a small number of essential variables are sufficient, in general less than in order to describe the initial state. From this observation one is inspired to look for a function which gives a correlation between Fourier modes such that the number of independent Fourier modes on the attractor is reduced.

The point of view developed by Kolmogorov [1941] is that the phenomena underlying for example turbulence are essentially finite-dimensional, although the dimension can be very large. The idea is that there is some finite set of essential modes or degrees of freedom which effectively govern the behavior while the remaining infinitely many degrees of freedom simply respond passively [Swinney & Gollub, 1985; Manneville, 1990]. This point of view is justified by the following observations. The infinite-dimensionality of the state space arises from the possibility of exciting disturbances of arbitrarily small spatial dimensions. On the other hand the frictional mechanism becomes very strong as the size of the disturbances becomes very small, so that they are damped out. A problem which attracts much attention is to characterize the “essential” modes and to find the slaving function which expresses, asymptotically in time, the “remaining” modes in terms of the “essential” modes.

The principle of slaving has been introduced in 1975 in the theory of synergetics by Haken (see Haken [1983]). It states that in the neighborhood of bifurcation points, where the system can change from one state to another, its behavior is characterized by a small number of Fourier modes. The slaving principle results from a hierarchy of time scales generated by the system near the instability. The time scales are derived from a linearization of the system in a neighborhood of the attractor. On the basis of the linearized problem, the set of Fourier modes is split up into a set of stable and a set of unstable modes. The time-scales of the stable modes are very small compared to those of the unstable modes. The very fast damping of the stable modes leads to a slaving of stable modes to unstable ones.

As a generalization of the slaving principle in the theory of synergetics, the theory of inertial manifolds and approximate inertial manifolds has been developed (see e.g., Temam [1988]). But while synergetics seeks a slaving function in the vicinity of a reference state, the theory of inertial manifolds tries to do so without a priori knowledge of a reference state.

Nonlinear Galerkin methods are new discretization methods to realize such approximations. A number of publications [Foias *et al.*, 1988b; Jauberteau *et al.*, 1989/90; Temam, 1991; Dubois *et al.*, 1991] suggest that they are more efficient than traditional, or linear, Galerkin methods.

The theory of inertial manifolds has been developed with the aim to provide a function that expresses high Fourier modes in terms of low ones, asymptotically in time [Temam, 1988; Temam, 1990; Foias *et al.*, 1988a; Foias *et al.*, 1988c; Foias *et al.*, 1988]. An IM  $\mathcal{M} \subset H$ , where  $H$  is an appropriate Hilbert space, for a dissipative PDE is a finite-dimensional smooth (Lipschitz) manifold which is positively invariant under the solution operator and uniformly attracts all trajectories at an exponential rate. It contains the global attractor, whenever it exists. However, for PDEs like the NSE and the MHD equations the existence of IMs is still an open problem.

Many PDEs, including the NSE and the MHD equations, can be written as abstract evolution equations in the Hilbert space  $H$ ,

$$\frac{du}{dt} + Au + B(u) = f, \quad (1)$$

where  $f \in H$ ,  $A$  is a linear, self-adjoint, positive operator in  $H$  and  $B$  a nonlinear operator in  $H$ . We assume that the initial-value problem for Eq. (1) is well-posed, i.e. that for all  $u_0 \in H$  there exists a unique solution of Eq. (1), satisfying the initial condition  $u(t=0) = u_0$ . In most applications  $A^{-1}$  is self-adjoint and compact and, therefore, there exists a complete orthonormal system of eigenvectors  $\{v_j\}_{j=1}^{\infty}$  of  $A$  in  $H$ :

$$Av_j = \lambda_j v_j, \quad j \in \mathbb{N},$$

$$0 < \lambda_1 \leq \lambda_2, \dots, \quad \lambda_j \rightarrow \infty \text{ as } j \rightarrow \infty.$$

Every solution  $u = u(t)$  to the initial value problem defined by Eq. (1) can be decomposed in this orthonormal basis,

$$u(t) = \sum_{j=1}^{\infty} \gamma_j(t) v_j. \quad (2)$$

For a given  $m \in \mathbb{N}$  we denote by  $P_m$  the projector in  $H$  onto the finite-dimensional subspace spanned by the eigenvectors  $v_1, v_2, \dots, v_m$  (the lower modes) and by  $Q_m = Id - P_m$  the projector onto the infinite-dimensional subspace spanned by the remaining eigenvectors (the higher modes). An IM is searched as the graph of a Lipschitz-continuous function  $\Phi_{IM} : P_m H \rightarrow Q_m H$  such that for every solution  $u$  to Eq. (1) with initial value on the IM there holds

$$Q_m u(t) = \Phi_{IM}(P_m u(t)) \quad \forall t \geq 0. \quad (3)$$

Since  $Q_m u(t)$  corresponds to small lengthscales, one can then say that the small scales are slaved to the large ones.

According to a definition introduced by Foias and Prodi [1967],  $m$  is called number of determining modes if for any two solutions  $u_1, u_2$  to Eq. (1)

$$\lim_{t \rightarrow \infty} |p_1 - p_2| = 0 \quad \text{implies} \quad \lim_{t \rightarrow \infty} |q_1 - q_2| = 0,$$

where  $p_i = P_m u_i$ ,  $q_i = Q_m u_i$  and  $u_i = p_i + q_i$  ( $i = 1, 2$ ). This criterion is clearly satisfied for solutions on an IM, since in this case

$$\lim_{t \rightarrow \infty} |q_1 - q_2| = \lim_{t \rightarrow \infty} |\Phi_{IM}(p_1) - \Phi_{IM}(p_2)| \leq l \lim_{t \rightarrow \infty} |p_1 - p_2|,$$

with  $l$  denoting a Lipschitz constant of  $\Phi_{IM}$ . Because of the exponential rate of attraction of an IM, the PDE can be approximated by a finite system of ODEs to calculate the solutions in the infinite-time limit.

For several PDEs, as for example the Kuramoto–Sivashinsky, Cahn–Hilliard and Ginzburg–Landau equations, the existence of an IM has been proven [Temam, 1988; Foias *et al.* 1988c; Foias *et al.* 1988]. But even if an IM exists, it is not necessarily found in a closed form as the graph of an explicit function  $\Phi_{IM}$ . Therefore the concept of approximate inertial manifolds (AIMs) has been introduced [Foias *et al.*, 1988b; Jolly *et al.* 1990; Titi, 1990]. An AIM is

actually an approximation of the solutions of a PDE for sufficiently large time and applicable regardless of the existence of an IM. Foias *et al.* [1988b] have used the smallness of the higher modes in the limit of large time to construct an AIM for the 2D NSE in the following way: Eq. (1) can be written as a coupled system of equations for  $p = P_m u$  and  $q = Q_m u$ ,

$$\frac{dp}{dt} + Ap + P_m B(p+q) = P_m f , \quad (4)$$

$$\frac{dq}{dt} + Aq + Q_m B(p+q) = Q_m f . \quad (5)$$

Foias *et al.* [1988b] could show that, since  $|q|$  and  $|dq/dt|$  remain small for large time, a reasonable approximation to Eq. (5) is given by

$$Aq + Q_m B(p) = Q_m f . \quad (6)$$

This led them to introduce a nonlinear function  $\Phi_{AIM} : P_m H \rightarrow Q_m H$  by

$$\Phi_{AIM}(p) := A^{-1}(Q_m f - Q_m B(p)) , \quad (7)$$

which defines an AIM

$$\mathcal{M} := \{\tilde{p} + \Phi_{AIM}(\tilde{p}) : \tilde{p} \in P_m H\} .$$

It represents the small-scale components  $q$  in an approximative way as a function of the large-scale components  $p$  of the solution. Any solution  $u = p + q$  to the 2D NSE satisfies

$$\limsup_{t \rightarrow \infty} |q(t) - \Phi_{AIM}(p(t))| \leq \varepsilon_m ,$$

where the constants  $\varepsilon_m$  tend to zero much faster than  $\limsup_{t \rightarrow \infty} |q(t)|$ . In a similar way an AIM for the 2D and 3D MHD equations has been constructed [Schmidtman, 1996a,b].

The linear Galerkin method projects Eq. (1) onto a finite-dimensional linear subspace  $P_m H$ . All terms in the orthogonal subspace  $Q_m H$  are small and are therefore neglected. One then looks for solutions  $u_m(t) \in P_m H$  to the following system of  $m$  ODEs:

$$\frac{du_m}{dt}(t) + Au_m(t) + P_m B(u_m(t)) = P_m f . \quad (8)$$

In nonlinear Galerkin methods the influence of small-scale structures of the flow on large-scale structures is captured by means of the AIM. Since the range of the nonlinear function  $\Phi_{AIM}$  is infinite-dimensional, it is necessary to truncate it for numerical calculations. This can be done by using  $P_n - P_m$ ,  $n > m$ , instead of  $Q_m$ . The AIM given by  $\Phi_{AIM}$  (see Eq. (7)) leads to

$$\frac{du_m}{dt}(t) + Au_m(t) + P_m B(u_m(t) + z_m(t)) = P_m f , \quad (9)$$

where  $u_m(t) \in P_m H$  and  $z_m(t) \in (P_n - P_m)H$ ,  $n > m$ , solves the truncated form of Eq. (6),

$$Az_m(t) + (P_n - P_m)B(u_m(t)) = (P_n - P_m)f , \quad (10)$$

which models the small scales  $z_m(t)$  as a function of the large scales  $u_m(t)$  [Jones & Titi, 1994; Jauberteau *et al.*, 1989/90].  $z_m(t) = 0$  corresponds to the linear Galerkin scheme given by Eq. (8). Theoretical studies have indicated that nonlinear Galerkin methods improve the

approximation of the exact solutions compared with simple linear truncations [Goubet, 1993; Jones *et al.* 1995; Devulder & Marion, 1992; Devulder *et al.*, 1993; Graham *et al.*, 1993].

In Sec. 2 we introduce the MHD equations and describe the implementation of Galerkin approximations. Then in Sec. 3 we present our numerical results and compare critical parameter values for bifurcations, convergence rates and computational efficiency, as well as energies, entropies and Kaplan–Yorke dimensions in the chaotic regime, for linear and nonlinear Galerkin methods. Sec. 4, finally, gives a short conclusion.

## 2 MHD Equations and Implementation of Galerkin Methods

The equations we are interested in are given in a domain  $\Omega \subset \mathbb{R}^3$ , occupied by a non-relativistic, incompressible, viscous fluid with finite electrical conductivity. The unknown functions are the fluid velocity  $\mathbf{u}$ , the magnetic field  $\mathbf{B}$  and the thermal pressure  $p$ . The density is supposed to be homogeneous and for simplicity set equal to unity. Then the equations can be written as [Roberts, 1967; Sermange & Temam, 1983]

$$\frac{\partial \mathbf{u}}{\partial t} + (\mathbf{u} \cdot \nabla) \mathbf{u} - \nu \cdot \Delta \mathbf{u} + \text{grad } p + \frac{1}{2} \text{grad } \mathbf{B}^2 - (\mathbf{B} \cdot \nabla) \mathbf{B} = \mathbf{f} \quad \text{in } \Omega, \quad (11)$$

$$\frac{\partial \mathbf{B}}{\partial t} + (\mathbf{u} \cdot \nabla) \mathbf{B} - (\mathbf{B} \cdot \nabla) \mathbf{u} - \eta \cdot \Delta \mathbf{B} = 0 \quad \text{in } \Omega, \quad (12)$$

$$\text{div } \mathbf{u} = 0 \quad \text{in } \Omega, \quad \text{div } \mathbf{B} = 0 \quad \text{in } \Omega, \quad (13)$$

where  $\nu$  and  $\eta$  denote kinematic viscosity and magnetic diffusivity (both assumed constant), and  $\mathbf{f}$  is an externally applied volume force. Eqs. (11)–(13) are completed by initial and boundary conditions upon  $\mathbf{u}$  and  $\mathbf{B}$ . We restrict ourselves to the case of periodic boundary conditions,

$$\left. \begin{aligned} \mathbf{u}(\mathbf{x} + 2\pi \mathbf{e}_i, t) &= \mathbf{u}(\mathbf{x}, t), \quad \mathbf{B}(\mathbf{x} + 2\pi \mathbf{e}_i, t) = \mathbf{B}(\mathbf{x}, t) \quad \mathbf{x} \in [0, 2\pi]^3, \\ \frac{\partial \mathbf{u}_j}{\partial x_k}(\mathbf{x} + 2\pi \mathbf{e}_i, t) &= \frac{\partial \mathbf{u}_j}{\partial x_k}(\mathbf{x}, t), \quad \frac{\partial \mathbf{B}_j}{\partial x_k}(\mathbf{x} + 2\pi \mathbf{e}_i, t) = \frac{\partial \mathbf{B}_j}{\partial x_k}(\mathbf{x}, t) \quad \mathbf{x} \in [0, 2\pi]^3, \end{aligned} \right\} \quad (14)$$

where  $(\mathbf{e}_i)_{i=1}^3$  is an orthonormal basis of  $\mathbb{R}^3$ ,  $j, k = 1 \dots 3$ .

The mean values of  $\mathbf{u}$  and  $\mathbf{B}$ , and consequently also of  $\mathbf{f}$ , are assumed to vanish,

$$\int_{[0, 2\pi]^3} \mathbf{u} \, d^3 \mathbf{x} = \mathbf{0}, \quad \int_{[0, 2\pi]^3} \mathbf{B} \, d^3 \mathbf{x} = \mathbf{0}, \quad \int_{[0, 2\pi]^3} \mathbf{f} \, d^3 \mathbf{x} = \mathbf{0}. \quad (15)$$

The periodicity assumption implies that

$$\exp(i\mathbf{k} \cdot \mathbf{x}), \quad \mathbf{k} \in \mathbb{Z}^3$$

is a complete orthonormal system of eigenvectors of the Laplacian with eigenvalues

$$\lambda_{\mathbf{k}} = \mathbf{k}^2, \quad \mathbf{k} \in \mathbb{Z}^3,$$

and that the Fourier representations of  $\mathbf{u}$ ,  $\mathbf{B}$ ,  $p$ , and  $\mathbf{f}$ ,

$$\mathbf{u}(\mathbf{x}, t) = \sum_{\mathbf{k} \in \mathbb{Z}^3, \mathbf{k} \neq \mathbf{0}} \mathbf{u}_{\mathbf{k}}(t) \exp(i\mathbf{k} \cdot \mathbf{x}), \quad \mathbf{B}(\mathbf{x}, t) = \sum_{\mathbf{k} \in \mathbb{Z}^3, \mathbf{k} \neq \mathbf{0}} \mathbf{B}_{\mathbf{k}}(t) \exp(i\mathbf{k} \cdot \mathbf{x}), \quad (16)$$

$$p(\mathbf{x}, t) = \sum_{\mathbf{k} \in \mathbb{Z}^3, \mathbf{k} \neq 0} p_{\mathbf{k}}(t) \exp(i \mathbf{k} \cdot \mathbf{x}) , \quad \mathbf{f}(\mathbf{x}) = \sum_{\mathbf{k} \in \mathbb{Z}^3, \mathbf{k} \neq 0} \mathbf{f}_{\mathbf{k}} \exp(i \mathbf{k} \cdot \mathbf{x}) , \quad (17)$$

can be differentiated term by term with respect to the spatial coordinates. In Fourier space Eq. (13) takes the form

$$\mathbf{u}_{\mathbf{k}} \cdot \mathbf{k} = 0 , \quad \mathbf{B}_{\mathbf{k}} \cdot \mathbf{k} = 0 \quad (18)$$

and is automatically satisfied if we write

$$\mathbf{u}_{\mathbf{k}} = u_{\mathbf{k}}^{(1)} \mathbf{e}_{\mathbf{k}}^{(1)} + u_{\mathbf{k}}^{(2)} \mathbf{e}_{\mathbf{k}}^{(2)} , \quad \mathbf{B}_{\mathbf{k}} = B_{\mathbf{k}}^{(1)} \mathbf{e}_{\mathbf{k}}^{(1)} + B_{\mathbf{k}}^{(2)} \mathbf{e}_{\mathbf{k}}^{(2)} \quad \text{for } \mathbf{k} \neq 0, \quad (19)$$

with real ‘‘polarisation’’ unit vectors  $\mathbf{e}_{\mathbf{k}}^{(1)}$  ,  $\mathbf{e}_{\mathbf{k}}^{(2)}$  perpendicular to  $\mathbf{k}$ ,

$$\mathbf{e}_{\mathbf{k}}^{(i)} \cdot \mathbf{k} = 0, \quad \mathbf{e}_{\mathbf{k}}^{(1)} \cdot \mathbf{e}_{\mathbf{k}}^{(2)} = 0, \quad \mathbf{e}_{\mathbf{k}}^{(i)} \cdot \mathbf{e}_{\mathbf{k}}^{(i)} = 1, \quad \mathbf{e}_{-\mathbf{k}}^{(i)} = \mathbf{e}_{\mathbf{k}}^{(i)}, \quad i = 1, 2. \quad (20)$$

The last condition in Eq. (20) ensures that

$$\mathbf{u}_{-\mathbf{k}} = \mathbf{u}_{\mathbf{k}}^* , \quad \mathbf{B}_{-\mathbf{k}} = \mathbf{B}_{\mathbf{k}}^* \quad (21)$$

for real  $\mathbf{u}(\mathbf{x})$  and  $\mathbf{B}(\mathbf{x})$ ; an asterisk indicates the complex conjugate. By using these representations for  $\mathbf{u}_{\mathbf{k}}$  and  $\mathbf{B}_{\mathbf{k}}$  we furthermore get rid of both the thermal, grad  $p$ , and magnetic, grad  $\mathbf{B}^2/2$ , pressure terms in Eq. (11) and arrive at the following infinite-dimensional system of ODEs:

$$\frac{du_{\mathbf{k}}^{(j)}}{dt} = -\nu \mathbf{k}^2 u_{\mathbf{k}}^{(j)} - i \sum_{\substack{\mathbf{p} \in \mathbb{Z}^3 \\ \mathbf{p} \neq 0, \mathbf{k}}} \sum_{\alpha, \beta=1}^2 (\mathbf{e}_{\mathbf{p}}^{(\alpha)} \cdot \mathbf{e}_{\mathbf{k}}^{(j)}) (\mathbf{e}_{\mathbf{k}-\mathbf{p}}^{(\beta)} \cdot \mathbf{k}) \left[ u_{\mathbf{p}}^{(\alpha)} u_{\mathbf{k}-\mathbf{p}}^{(\beta)} - B_{\mathbf{p}}^{(\alpha)} B_{\mathbf{k}-\mathbf{p}}^{(\beta)} \right] + f_{\mathbf{k}}^{(j)} \quad (22)$$

$$\frac{dB_{\mathbf{k}}^{(j)}}{dt} = -\eta \mathbf{k}^2 B_{\mathbf{k}}^{(j)} - i \sum_{\substack{\mathbf{p} \in \mathbb{Z}^3 \\ \mathbf{p} \neq 0, \mathbf{k}}} \sum_{\alpha, \beta=1}^2 (\mathbf{e}_{\mathbf{p}}^{(\alpha)} \cdot \mathbf{e}_{\mathbf{k}}^{(j)}) (\mathbf{e}_{\mathbf{k}-\mathbf{p}}^{(\beta)} \cdot \mathbf{k}) \left[ B_{\mathbf{p}}^{(\alpha)} u_{\mathbf{k}-\mathbf{p}}^{(\beta)} - u_{\mathbf{p}}^{(\alpha)} B_{\mathbf{k}-\mathbf{p}}^{(\beta)} \right]. \quad (23)$$

$f_{\mathbf{k}}^j$  on the right of Eq. (22) is defined by

$$f_{\mathbf{k}}^j = \mathbf{f}_{\mathbf{k}} \cdot \mathbf{e}_{\mathbf{k}}^{(j)}, \quad j = 1, 2. \quad (24)$$

Because of the condition (21) we can restrict ourselves to  $\mathbf{k}$  vectors in a subset  $\mathcal{IK}$  of  $\mathbb{Z}^3$ , defined by

$$\mathcal{IK} := \{(k_1, k_2, k_3) \in \mathbb{Z}^3 : k_3 > 0\} \cup \{(k_1, k_2, 0) \in \mathbb{Z}^3 : k_1 > 0\} \cup \{(0, k_2, 0) \in \mathbb{Z}^3 : k_2 > 0\} .$$

It has been useful for our calculations to segment  $\mathcal{IK}$  into successive shells of  $\mathbf{k}$  vectors

$$\mathcal{IK}_i := \{\mathbf{k} \in \mathcal{IK} : \mathbf{k}^2 = i\} \quad i = 1, 2, \dots$$

$$\mathcal{IK} = \bigcup_{i=1}^{\infty} \mathcal{IK}_i ; \quad \mathcal{IK}_i \cap \mathcal{IK}_j = \emptyset , \quad i, j \in \mathbb{N}, \quad i \neq j.$$

An overview of the segmentation is given in the Appendix.

For linear Galerkin methods LGM( $m$ ) we restrict Eqs. (22)–(23) to a finite set of  $\mathbf{k}$  vectors such that  $\mathbf{k}$ ,  $\mathbf{p}$  and  $\mathbf{k} - \mathbf{p}$  belong to shells  $1 \dots m$ . To implement nonlinear Galerkin methods NLGM( $m, n$ ) we represent coefficients of wave vectors in shells  $m + 1 \dots n$ ,  $1 < m < n$  in terms of coefficients of wave vectors in shells  $1 \dots m$  according to the definition of  $\Phi_{AIM}$  (see Eq. (7)) by

$$u_{\mathbf{k}}^{(j)} := \frac{-i}{\nu \mathbf{k}^2} \sum_{\substack{\mathbf{p} \in \cup_{i=1}^m \mathbb{K}_i \\ \mathbf{p} \neq 0, \mathbf{k}}} \sum_{\alpha, \beta=1}^2 (\mathbf{e}_{\mathbf{p}}^{(\alpha)} \cdot \mathbf{e}_{\mathbf{k}}^{(j)}) (\mathbf{e}_{\mathbf{k}-\mathbf{p}}^{(\beta)} \cdot \mathbf{k}) \left[ u_{\mathbf{p}}^{(\alpha)} u_{\mathbf{k}-\mathbf{p}}^{(\beta)} - B_{\mathbf{p}}^{(\alpha)} B_{\mathbf{k}-\mathbf{p}}^{(\beta)} \right] + \frac{f_{\mathbf{k}}^{(j)}}{\nu \mathbf{k}^2}$$

and

$$B_{\mathbf{k}}^{(j)} := \frac{-i}{\eta \mathbf{k}^2} \sum_{\substack{\mathbf{p} \in \cup_{i=1}^m \mathbb{K}_i \\ \mathbf{p} \neq 0, \mathbf{k}}} \sum_{\alpha, \beta=1}^2 (\mathbf{e}_{\mathbf{p}}^{(\alpha)} \cdot \mathbf{e}_{\mathbf{k}}^{(j)}) (\mathbf{e}_{\mathbf{k}-\mathbf{p}}^{(\beta)} \cdot \mathbf{k}) \left[ B_{\mathbf{p}}^{(\alpha)} u_{\mathbf{k}-\mathbf{p}}^{(\beta)} - u_{\mathbf{p}}^{(\alpha)} B_{\mathbf{k}-\mathbf{p}}^{(\beta)} \right].$$

If we take  $\mathbf{p}$  and  $\mathbf{k}$  such that  $\mathbf{p}^2 \leq m$  and  $(\mathbf{k} - \mathbf{p})^2 \leq m$  we get

$$\mathbf{k}^2 = ((\mathbf{k} - \mathbf{p}) + \mathbf{p})^2 = (\mathbf{k} - \mathbf{p})^2 + 2(\mathbf{k} - \mathbf{p}) \cdot \mathbf{p} + \mathbf{p}^2 \leq 4m$$

and therefore we always choose  $n \leq 4m$ . Solutions to LGM( $m$ ) and NLGM( $m, n$ ) are denoted by  $\mathbf{u}_m, \mathbf{B}_m$ , while the correction terms for nonlinear Galerkin methods are  $\mathbf{z}_m$  for the velocity and  $\mathbf{Z}_m$  for the magnetic field ( $(\mathbf{z}_m, \mathbf{Z}_m) = \Phi_{AIM}(\mathbf{u}_m, \mathbf{B}_m)$ ).

We have used the forcing

$$\mathbf{f} = \nu \mathbf{u}_{ABC}, \quad (25)$$

where  $\mathbf{u}_{ABC}$  is an ABC flow (named after Arnold, Beltrami and Childress),

$$\mathbf{u}_{ABC}(x, y, z) = (A \sin k_0 z + C \cos k_0 y, B \sin k_0 x + A \cos k_0 z, C \sin k_0 y + B \cos k_0 x),$$

with  $A, B, C$  and  $k_0$  denoting constants (for a rather comprehensive account of the ABC flows see Dombre *et al.* [1986]). The ABC flows are Beltrami fields, namely,  $\text{curl } \mathbf{u}_{ABC} \times \mathbf{u}_{ABC} = \mathbf{0}$ ; thus they are strongly helical. In general (if  $ABC \neq 0$ ), there are domains in the flow where the streamlines are chaotic. Mainly for these two reasons, the ABC flows have received much interest in the context of kinematic dynamo theory (e.g., Galloway & Frisch [1986]).

The ABC flows are steady solutions of the incompressible Euler equation. They are also steady solutions of the incompressible NSE (Eq. (11) with the magnetic field dropped) if an external forcing as given by Eq. (25) is applied to compensate for viscous losses. The bifurcation properties of the NSE with ABC forcing have been investigated by Podvigina & Pouquet [1994], while studies of the MHD equations with this kind of forcing are due to Galanti *et al.* [1992], Feudel *et al.* [1995, 1996a,b] and Sehafer *et al.* [1996].

Throughout our calculations we have used a forcing according to Eq. (25) with

$$k_0 = 1, \quad A = B = C = f$$

and have, following Galanti *et al.* [1992], defined kinetic and magnetic Reynolds numbers  $R$  and  $Rm$  by

$$R = \frac{f}{\nu}, \quad Rm = \frac{f}{\eta}.$$

While restricting ourselves to the case  $\nu = \eta$  (magnetic Prandtl number equal to unity),  $R$  has been our bifurcation parameter.



### 3 Numerical Results

#### 3.1 Stationary solutions

For sufficiently weak forcing (small  $R$ ) the ABC flow with no magnetic field is the only attracting state. For varying  $R$  we have calculated the eigenvalues of the Jacobian in order to detect bifurcation points. If  $R$  is increased, the ABC flow loses stability in a Hopf bifurcation.

The steady state to LGM( $m$ ) loses stability in a Hopf bifurcation if  $m \geq 3$ , leading to a periodic solution with a nonvanishing magnetic field. As is seen in Fig. 1, the critical Reynolds number for the Hopf bifurcation,  $R_c$ , changes with increasing  $m$  as long as  $m \leq 37$ . For larger values of  $m$  the bifurcation point,  $R_c = 8.7$ , does not depend on  $m$ . This value of  $R_c$  coincides approximately with the critical Reynolds number for the magnetic instability in the corresponding kinematic dynamo problem, for which a value of  $R_c = 8.9$  has been found (cf. Galloway & Frisch [1986]).

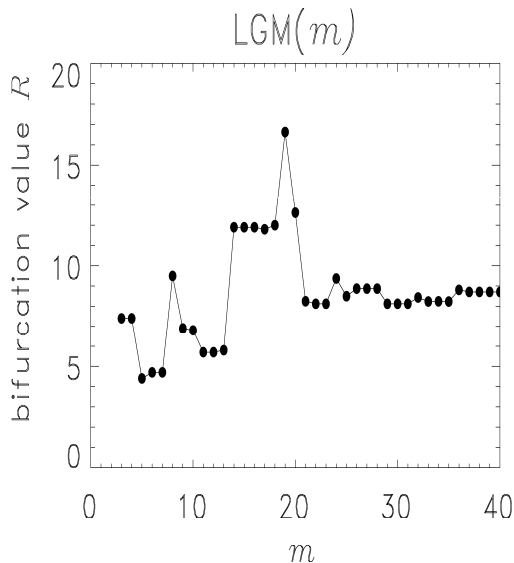


**Figure 1:** Hopf-bifurcation value of Reynolds number for LGM( $m$ ) versus number of shells  $m$ .

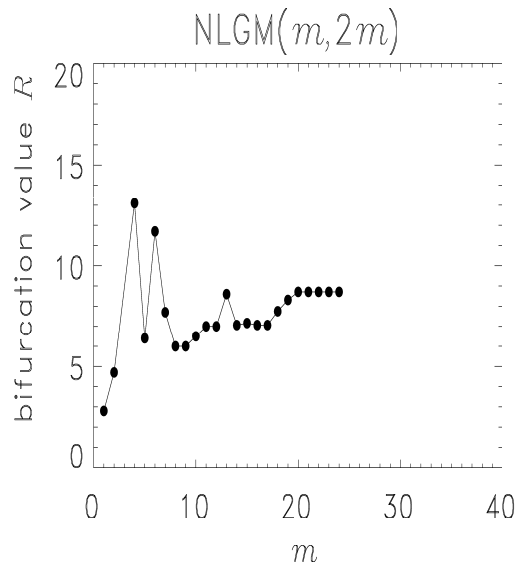


**Figure 2:** Hopf-bifurcation value of Reynolds number for NLGM( $m, 2m$ ) versus number of active shells  $m$ .

For NLGM( $m, 2m$ ) we observe a similar bifurcation behavior. However, the number of active shells necessary to obtain  $R_c = 8.7$  is smaller than for LGM( $m$ ). While we need 37 active shells for LGM( $m$ ), this number is reduced to 20 shells for NLGM( $m, 2m$ ) (see Fig. 2). We interpret the modes in shells  $1 \leq m \leq 20$  as determining modes and those in shells  $20 < m \leq 37$  as slaved modes.

#### 3.2 Accuracy and computational efficiency of nonlinear Galerkin methods

Next we have studied, for a periodic orbit, the influence of the degree of truncation on the quality of the approximation, both for the LGM and the NLGM. We have fixed the Reynolds number at  $R = 10$ , where a periodic attractor exists if  $m \geq 21$ , and have varied the number of shells taken

into account. The solution  $\mathbf{u}_{37}, \mathbf{B}_{37}$  obtained using LGM(37) has been taken as the “exact” solution (see Sec. 3.1) and the distance of other approximate trajectories from this reference solution has been measured. Starting from initial values  $\mathbf{u}_0 = P_7 \mathbf{u}_{37}(0)$  and  $\mathbf{B}_0 = P_7 \mathbf{B}_{37}(0)$ , we define the error  $\varepsilon_{LGM(m)}$  for a given number of shells ( $m \geq 21$ ) by

$$\varepsilon_{LGM(m)} = \max_{t \in [T_1, T_2]} \left( \|\mathbf{u}_{37}(t) - \mathbf{u}_m(t)\|_{L^2}^2 + \|\mathbf{B}_{37}(t) - \mathbf{B}_m(t)\|_{L^2}^2 \right), \quad (26)$$

where  $[T_1, T_2]$  is one period of  $\mathbf{u}_{37}, \mathbf{B}_{37}$ ;  $\varepsilon_{LGM(m)}$  is a measure for the distance between the nearly exact periodic orbit ( $m = 37$ ) and the corresponding approximate  $m$ -shell solution ( $21 \leq m \leq 37$ ).

Similarly the nonlinear Galerkin method NLGM( $m, 2m$ ) ( $m = 7 \dots 17$ ) has been used to approximate the same periodic orbit. As above, the initial values have been taken near the “exact” periodic solution calculated with LGM(37). The corresponding error is defined analogously to Eq. (26) by

$$\varepsilon_{NLGM(m, 2m)} = \max_{[T_1, T_2]} \left( \|\mathbf{u}_{37}(t) - (\mathbf{u}_m(t) + \mathbf{z}_m(t))\|_{L^2}^2 + \|\mathbf{B}_{37}(t) - (\mathbf{B}_m(t) + \mathbf{Z}_m(t))\|_{L^2}^2 \right). \quad (27)$$

We have measured both the accuracy of the approximation and the CPU time needed, so that each method corresponds to a point in the plane spanned by CPU time and accuracy. In Fig. 3 the accuracies  $\xi$  are drawn versus the CPU time needed. For larger  $m$ ,  $m > 15$ , the use of the nonlinear Galerkin methods allows a reduction of CPU time by approximately 30% compared to the linear methods.

### 3.3 Energy, enstrophy and Kaplan–Yorke dimension for the chaotic regime

To estimate the number of modes needed to describe the behavior of the exact solutions in the chaotic regime qualitatively correctly, we have furthermore calculated the energy of the flow,

$$\frac{1}{2} \|\mathbf{u}\|_{L^2}^2 + \frac{1}{2} \|\mathbf{B}\|_{L^2}^2 = \frac{1}{2} (2\pi)^3 \sum_{\mathbf{k} \in \mathbb{Z}^3} (|\mathbf{u}_{\mathbf{k}}|^2 + |\mathbf{B}_{\mathbf{k}}|^2),$$

as well as its enstrophy,

$$\|\operatorname{curl} \mathbf{u}\|_{L^2}^2 + \|\operatorname{curl} \mathbf{B}\|_{L^2}^2,$$

which, because of periodic boundary conditions, satisfies (cf. Doering & Gibbon [1995])

$$\|\nabla \mathbf{u}\|_{L^2}^2 + \|\nabla \mathbf{B}\|_{L^2}^2 = (2\pi)^3 \sum_{\mathbf{k} \in \mathbb{Z}^3} \mathbf{k}^2 (|\mathbf{u}_{\mathbf{k}}|^2 + |\mathbf{B}_{\mathbf{k}}|^2).$$

In Schmidtman [1996] the number of determining modes for the MHD equations has been estimated.  $m_0$  is number of determining modes if

$$\lambda_{m_0+1} > c_0 \left( \frac{M}{\nu} \right)^2, \quad (28)$$

where

$$M := \lim_{t \rightarrow \infty} \sup \frac{1}{t} \int_0^t \|\nabla \mathbf{u}(\tau)\|_{L^2}^2 + \|\nabla \mathbf{B}(\tau)\|_{L^2}^2 d\tau \quad \text{and} \quad c_0 = \text{const} > 0,$$

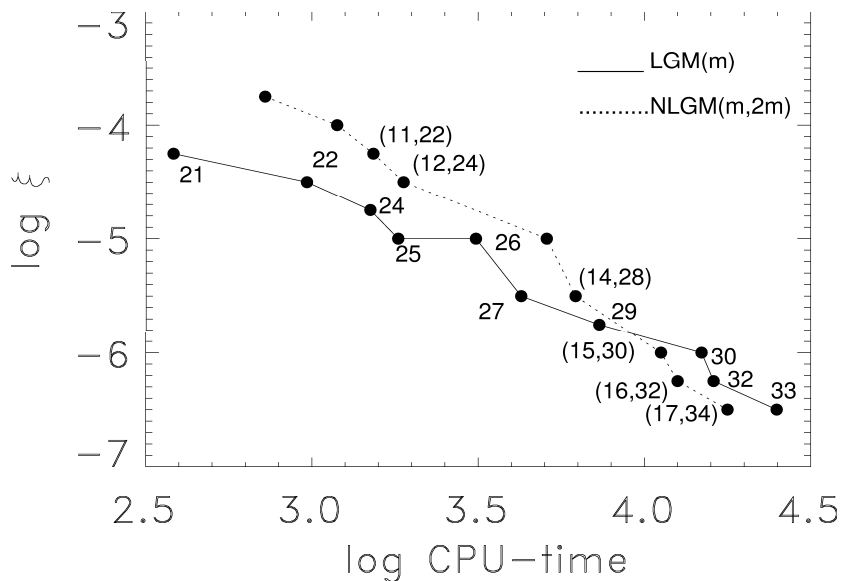


**Figure 3:** CPU time to approximate  $\mathbf{u}_{37}, \mathbf{B}_{37}$  with accuracy  $\xi$  for linear Galerkin methods  $\text{LGM}(m)$  and nonlinear Galerkin methods  $\text{NLGM}(m, 2m)$  ( $R = 10$ ).

what shows that enstrophy decisively influences the number of determining modes.

The following numerical experiments have been done for a Reynolds number of 20, for which the solutions are chaotic. Their chaotic character has been verified by calculating the Lyapunov exponents.

In Figs. 4 and 5 energy and enstrophy of the flow are given as functions of the numbers of shells. As can be seen from Figs. 4 and 5, for  $\text{LGM}(m)$   $m^* = 35$  is a saturation point with respect to the calculation of both energy and enstrophy, in the sense that for further increasing  $m$  both quantities do not change significantly. If the constant  $c_0$  in Eq. (28) would be known (actually it is unknown), the saturation value of the enstrophy could be used to estimate the number of determining modes. As can be seen in Figs. 6 and 7, by applying  $\text{NLGM}(l, 35)$  the saturation point is shifted to a smaller number,  $l$ , of (active) shells.

By using an algorithm of Shimada and Nagashima [1979], for  $R = 20$  the largest Lyapunov exponents have been computed and used to calculate the Kaplan–Yorke dimension  $D_{KY}$  of the attractor, which provides a good approximation of its Hausdorff dimension [Kaplan & Yorke, 1979].

If the Lyapunov exponents  $\mu_i$  are ordered descendingly and  $j$  is the largest index satisfying

$$\sum_{i=1}^j \mu_i \geq 0,$$

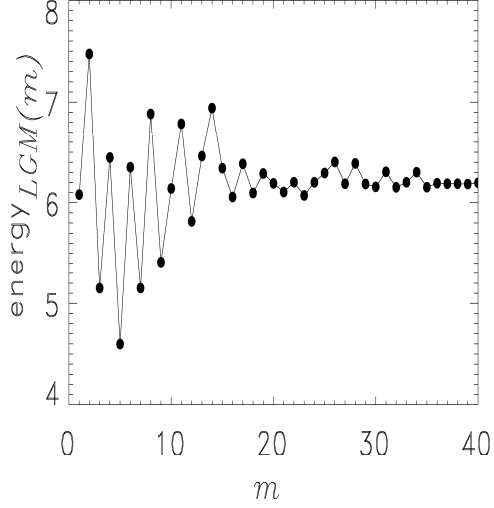


**Figure 4:** Time average of energy versus number of shells  $m$  containing the active modes for LGM( $m$ ) ( $R = 20$ ).

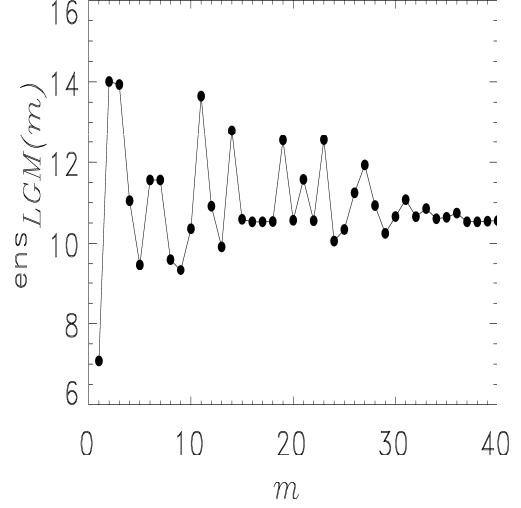


**Figure 5:** Time average of enstrophy versus number of shells  $m$  containing the active modes for LGM( $m$ ) ( $R = 20$ ).

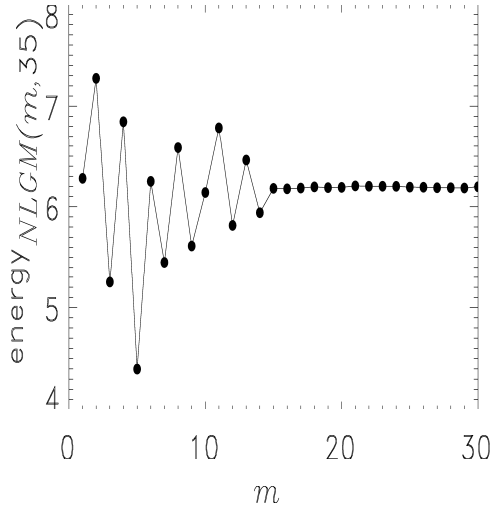


**Figure 6:** Time average of energy versus number of shells  $m$  containing the active modes for NLGM( $m, 35$ ) ( $R = 20$ ).

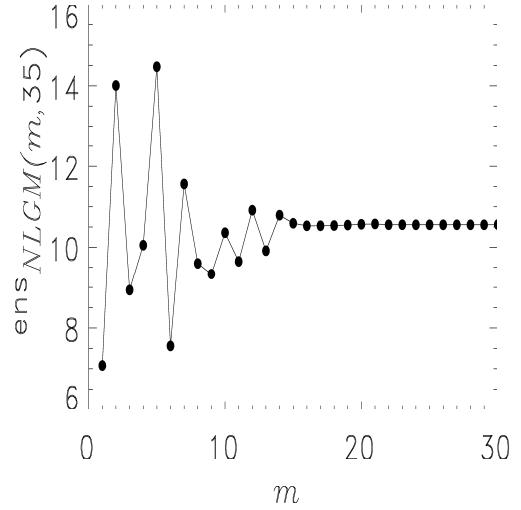


**Figure 7:** Time average of enstrophy versus number of shells  $m$  containing the active modes for NLGM( $m, 35$ ) ( $R = 20$ ).

then

$$D_{KY} = j - \frac{\sum_{i=1}^j \mu_i}{|\mu_{j+1}|}.$$

Fig. 8 gives the Kaplan–Yorke dimensions calculated by means of LGM and NLGM versus the number of active shells. With LGM a saturation is reached at  $m = 14$  (while the saturation with respect to energy and enstrophy is reached at  $m = 35$ ). With nonlinear Galerkin method NLGM( $l, 14$ ) the plateau value of the Kaplan–Yorke dimension is reasonably approximated already for  $l = 10$ . This again suggest that the constructed map  $\phi_{AIM}$  provides an acceptable approximation of the small-scale structures of the flow. By means of NLGM(10, 14) we can reduce the CPU time needed to calculate the dimension of the attractor compared to LGM(14) by 25%.

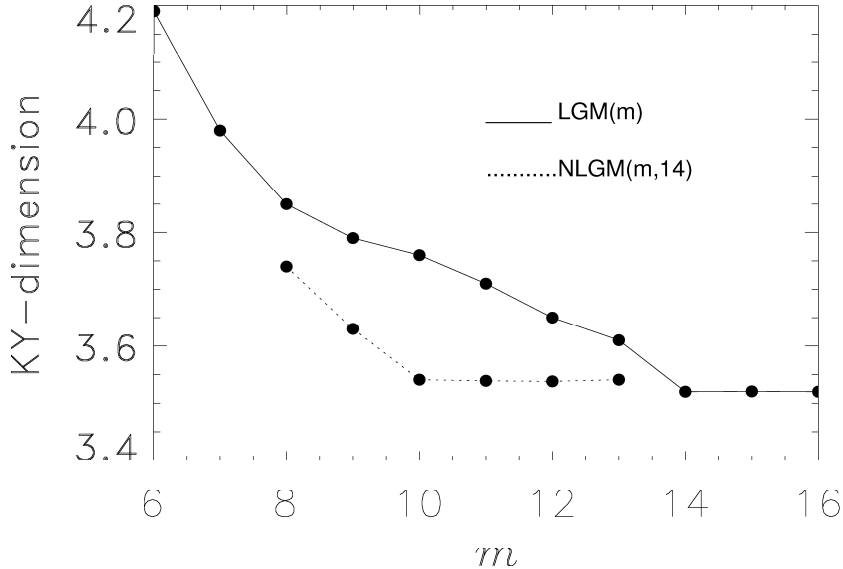


**Figure 8:** Kaplan–Yorke dimension versus number of active shells for LGM( $m$ ) and NLGM( $m, 14$ ) ( $R = 20$ ).

## 4 Conclusion

In this paper we have investigated the problem of approximating the long-term behavior of solutions to the 3D MHD equations by both linear and nonlinear Galerkin methods. Since there exists a finite number of determining modes for the equations, one expects to be able to enslave higher modes by some nonlinear function. We have constructed such a nonlinear function  $\Phi_{AIM}$ , an approximate inertial manifold, for the MHD case similar to the one introduced by Foias, Manley and Temam [1988b] for the NSE and have implemented a nonlinear Galerkin method based on the approximate inertial manifold. Special bifurcation points, averaged values of energy and enstrophy as well as the Kaplan–Yorke dimension have been calculated for both linear and nonlinear Galerkin methods in order to estimate the number of modes necessary to

correctly describe the behavior of the exact solutions. Compared to the linear methods, the nonlinear methods admit a reduction of the number of active modes and saves additionally computational costs (CPU time).

## Acknowledgments

This work was supported in part by the Deutsche Forschungsgemeinschaft (DFG) under its main topic “Ergodentheorie, Analysis und effiziente Simulation dynamischer Systeme”.

## References

- Constantin P. & Foias C. [1985] “Global Lyapunov exponents, Kaplan–Yorke formulas and the dimension of attractors for the 2–dimensional Navier–Stokes equations,” *Comm. Pure Appl. Math.* **XXXVIII**, 1–27.
- Constantin P., Foias C., Manley O. & Temam R. [1985] “Determining modes and fractal dimension of turbulent flows,” *J. Fluid Mech.* **150**, 427–440.
- Devulder C. & Marion M. [1992] “A class of numerical algorithms for large time integration: the nonlinear Galerkin methods,” *SIAM J. Numer. Anal.* **29**, 462–483.
- Devulder C., Marion M. & Titi E. [1993] “On the rate of convergence of the nonlinear Galerkin methods,” *Math. Comp.* **60**, 495–514.
- Doering C. & Gibbon J. [1995] *Applied Analysis of the Navier–Stokes equations*. (University Press, Cambridge).
- Dombre T., Frisch U., Greene J., Hénon M., Mehr A. & Soward A. [1986] “Chaotic streamlines in the ABC flow,” *J. Fluid Mech.* **167**, 353–391.
- Dubois T., Jaubertau F., Marion F. & Temam R. [1991] “Subgrid modelling and interaction of small and large wavelengths in turbulent flows,” *Comput. Phys. Commun.* **65**, 100–106.
- Feudel F., Seehafer N., Galanti B. & Rüdiger S. [1996] “Symmetry–breaking bifurcations for the magnetohydrodynamic equations with helical forcing,” *Phys. Rev.* **E 54**, 2589–2596.
- Feudel F., Seehafer N. & Schmidtman O. [1995a] “Bifurcation Phenomena of the Magnetofluid Equations,” *Mathematics and Computers in Simulation* **40(3)**, 235–246.
- Feudel F., Seehafer N. & Schmidtman O. [1995b] “Fluid helicity and dynamo bifurcations,” *Physics Letters A* **202**, 73–78.
- Foias C., Jolly M., Kevrekidis I., Sell G. & Titi E. [1988a] “On the computation of inertial manifolds,” *Physics Letters A* **131, No. 7; 8**, 433–436.
- Foias C., Manley O. & Temam R. [1988b] “Modelling of the interaction of small and large eddies in two dimensional turbulent flows,” *Mathematical Modelling and Numerical Analysis* **22**, 93–114.

- Foias C., Nicolaenko B., Sell G. & Temam R. [1988c] “Inertial manifolds for the Kuramoto–Sivashinsky equation and an estimate of their lowest dimension,” *J. Math. Pures Appl.* **67**, 197–226.
- Foias C. & Prodi G. [1967] “Sur le comportement global des solutions non stationnaires des équations de Navier–Stokes on Dimensional 2,” *Rend. Sem. Mat. Univ. Padova* **39**, 1.
- Foias C., Sell G. & Temam R. [1988] “Inertial manifolds for nonlinear evolutionary equations,” *J. Diff. Eqns.* **73**, 309–353.
- Galanti B., Sulem P. & Pouquet A. [1992] “Linear and non-linear dynamos associated with ABC flows,” *Geophys. Astrophys. Fluid Dyn.* **66**, 183–208.
- Galloway D. & Frisch U. [1986] “Dynamo action in a family of flows with chaotic streamlines,” *Geophys. Astrophys. Fluid Dyn.* **36**, 53–83.
- Goubet O. [1993] “Nonlinear Galerkin methods using hierarchical almost-orthogonal finite elements bases,” *Nonlinear Analysis* **20**, No.3, 223–247.
- Graham M., Steen P. & Titi E. [1993] “Computational efficiency and approximate inertial manifolds for a Bénard convection system,” *J. Nonlin. Sci.* **3**, 153–167.
- Haken H. [1993] *Advanced Synergetics*. (Springer, Berlin).
- Jauberteau F., Rosier C. & Temam R. [1989/90] “The nonlinear Galerkin method in computational fluid mechanics,” *Applied Numerical Mathematics* **6**, 361–370.
- Jolly M., Kevrekidis I. & Titi E. [1990] “Approximate inertial manifolds for the Kuramoto–Sivashinsky equation: analysis and computations,” *Physica D* **44**, 38–60.
- Jones D., Margolin L. & Titi E. [1995] “On the effectiveness of the approximate inertial manifold—a computational study,” *Theoretical and Computational Fluid Dynamics* **7**, No.4, 243–260.
- Jones D. & Titi E. [1994] “A remark on quasi-stationary approximate inertial manifolds for the Navier–Stokes equations,” *SIAM J. Math. Anal.* **25**, No.3, 894–914.
- Kaplan J. & Jorke J. [1979] “Chaotic behavior of multidimensional difference equations,” *In Functional Differential Equations and Approximations of Fixed Points, H.O. Peitgen and H.O. Walthers (eds.), Springer Lecture Notes in Mathematics, Springer Verlag: Berlin* **730**, 228–237.
- Kolmogorov A. [1941a] “The local structure of turbulence in an incompressible fluid with very large Reynolds numbers,” *Dokl. Akad. Nauk SSSR* **30**, 301–305.
- Kolmogorov A. [1941b] “On the degeneration of isotropic turbulence in an incompressible viscous fluid,” *Dokl. Akad. Nauk SSSR* **31**, 538–540.
- Manneville P. [1990] *Dissipative Structures and Weak Turbulence*. (Academic Press, London).
- Marion M. & Temam R. [1989] “Nonlinear Galerkin methods,” *SIAM J. Num. Anal.* **26** No.5, 1139–1157.

- Podvigina O. & Pouquet A. [1994] “On the non-linear stability of the 1:1:1 ABC flow,” *Physica D* **75**, 471–508.
- Roberts P. [1967] *An Introduction to Magnetohydrodynamics*. (Longmans, London).
- Schmidtman O. [1996] “Modelling of the interaction of lower and higher modes in two-dimensional MHD equations,” *J. Nonlin. Anal.* **26**,No.1, 41–54.
- Schmidtman O. [April 1996] *Nichtlineare Galerkin-Verfahren für die 3D magnetohydrodynamischen Gleichungen*. (Dissertation, Universität Potsdam).
- Seehafer N., Feudel F. & Schmidtman O. [1996] “Nonlinear dynamo with ABC forcing,” *Astron. Astrophys.* **36**, 693–699.
- Sermange M. & Temam R. [1983] “Some mathematical questions related to the MHD equations,” *Comm. Pure Appl. Math.* **36**, 635–664.
- Shimada I. & Nagashima T. [1979] “A numerical approach to ergodic problem of dissipative dynamical systems,” *Progr. Theor. Phys.* **61**(6), 1605–1616.
- Swinney H. & Gollub J. [1985] *Hydrodynamic Instabilities and the Transition to Turbulence*. (Springer Verlag, Berlin).
- Temam R. [1988] *Infinite Dimensional Dynamical Systems in Mechanics and Physics*. (Springer, New York).
- Temam R. [1990] “Inertial manifolds,” *The Mathematical Intelligencer* **12** (4), 68–74.
- Temam R. [1991] “Stability analysis of the nonlinear Galerkin method,” *Mathematics of Computations* **57**,No.196, 477–505.
- Temam R. [1995] *Navier–Stokes Equations and Nonlinear Funktional Analysis*. (CBMS Regional Conference Series, No.66, SIAM, Philadelphia).
- Titi E. [1990] “On approximate inertial manifolds to the Navier–Stokes equations,” *J. Math. Anal. Appl.* **149**, 540–557.

## Appendix

Table 1 gives an overview of the partition of  $\mathbf{k}$  space into successive disjoint shells of  $\mathbf{k}$  vectors.



Number $m$ of shell in $\mathbf{k}$ space	Number of $\mathbf{k}$ vectors in shell $\mathbb{K}_m$	Number of $\mathbf{k}$ vectors in $\cup_{j=1}^m \mathbb{K}_j$	Number of ODEs for LGM( $m$ )
1	3	3	24
2	6	9	72
3	4	13	104
4	3	16	128
5	12	28	224
6	12	40	320
7	0	40	320
8	6	46	368
9	15	61	488
10	12	73	584
11	12	85	680
12	4	89	712
13	12	101	808
14	24	125	1000
15	0	125	1000
16	3	128	1024
17	24	152	1216
18	18	170	1360
19	12	182	1456
20	12	194	1552
21	24	218	1744
22	12	230	1840
23	0	230	1840
24	12	242	1936
25	15	257	2056
26	36	293	2344
27	16	309	2472
28	0	309	2472
29	36	345	2760
30	24	369	2952
31	0	369	2952
32	6	375	3000
33	24	399	3192
34	24	423	3384
35	24	447	3576
36	15	462	3696
37	12	474	3792
38	36	510	4080
39	0	510	4080
40	12	522	4176

**Table 1:** Partition of  $\mathbf{k}$  space.